

### South-North dipole in summer precipitation over Northeast China

Xinya Shu<sup>1</sup> · Shanshan Wang<sup>1,2</sup> D · Hao Wang<sup>1</sup> · Yuanyuan Hu<sup>1</sup> · Yiwei Pang<sup>1</sup> · Jianping Huang<sup>1,2</sup>

Received: 16 January 2024 / Accepted: 24 April 2024 / Published online: 6 May 2024 © The Author(s), under exclusive licence to Springer-Verlag GmbH Germany, part of Springer Nature 2024

#### **Abstract**

This study discusses the interannual variability and influencing mechanisms of the summer precipitation dipole pattern in Northeast China from 1961 to 2020 based on observation data and reanalysis data. Results indicate that the second mode of empirical orthogonal function (EOF2) mode of summer (June–August) precipitation in Northeast China presents a dipole pattern with opposite trends in the north and south, and its time series (PC2) demonstrates significant interannual variations. The South-North dipole pattern in summer precipitation over Northeast China are significantly correlated with the tropical sea surface temperature, Arctic sea ice, and Eurasian snow cover in the preceding spring (March–May) on an interannual scale. In the preceding spring, the rise in sea temperature in the eastern equatorial Pacific and the decline in the western equatorial Pacific can stimulate EAP and EU teleconnections, positioning a cyclonic center over Northeast China, thereby influencing the dipole pattern of precipitation in Northeast China. Furthermore, the anomalies in European snow cover and Arctic sea ice can lead to an increase in albedo and a decrease in upward heat flux, causing the lower atmospheric temperature to drop and persist into the summer. This triggers the eastward propagation of atmospheric Rossby waves at mid-high latitudes, which promotes precipitation in Northeast China through the occurrence of negative potential height anomalies. These conditions influence the anomalies in the atmospheric circulation over the Eurasian continent, regulate moisture transport and vertical motion, and collectively contribute to the dipole pattern of summer precipitation in Northeast China over the past 60 years, with opposite trends in the north and south.

 $\textbf{Keywords} \ \ Northeast \ summer \ precipitation \cdot Dipole \ mode \cdot Decadal \ trend \cdot Circulation \ characteristics \cdot Physical \ mechanism$ 

Shanshan Wang wangss@lzu.edu.cn

Xinya Shu 220220903180@lzu.edu.cn

Hao Wang wangh21@lzu.edu.cn

Yuanyuan Hu huyy2023@lzu.edu.cn

Yiwei Pang pangyw2023@lzu.edu.cn

- Key Laboratory for Semi-Arid Climate Change of the Ministry of Education, College of Atmospheric Sciences, Lanzhou University, Lanzhou 730000, China
- Collaborative Innovation Center for Western Ecological Safety, Lanzhou University, Lanzhou 730000, China

#### 1 Introduction

Northeast China (NEC, 38–55°N, 110–135°E) is located in eastern Asia and serves as one of the crucial grain production bases in China. This monsoonal region experiences considerable variability in precipitation distribution, making it susceptible to severe drought and torrential rainfall, particularly during the summer. Understanding the historical characteristics, variability of precipitation, and the governing rules of this precipitation variability is therefore of utmost importance.

Numerous studies have examined the annual and summer precipitation in NEC, revealing that the region's precipitation is influenced by both local internal atmospheric variability and extrinsic forcing through teleconnections. These include the Northeast cold vortex (NECV) (Sun and An 2001; Wang et al. 2007), the East Asian summer monsoon (Sun et al. 2017), sea surface temperature (SST) anomaly (Han et al. 2015), snow conditions over the Tibetan Plateau and Eurasian (Wu et al. 2009a, b), and Arctic sea ice (Li et al. 2018), etc. Among these, the NECV is a crucial factor affecting



NEC's summer precipitation, with precipitation generally increasing with NECV strengthening (Liu et al. 2002; Gao and Gao 2018). Based on previous studies, we have found that the summer precipitation in the eastern and northeastern regions of China is characterized by significant circulation features of low-pressure systems (Cao et al. 2018; Zhao et al. 2018; Chen and Zhang 2020). Therefore, this study will primarily focus on the impact of low-pressure systems on precipitation. Further, preceding SST anomalies in key areas, including the equatorial Pacific relate to El Niño-Southern Oscillation (ENSO) (Han et al. 2017; Feng and Li 2011), the southwest Indian Ocean (Feng et al. 2017; Xie et al. 2020) and the North Atlantic and equatorial Atlantic Ocean (Sun et al. 2015; Li et al. 2020a, b), can influence the NECV-related precipitation by exciting the atmospheric circulation anomaly (Fang et al. 2018). For instance, ENSO, as a strong signal of ocean-atmosphere interaction, is considered as a major factor for NEC precipitation variability. Sun and Wang (2006) suggested that SST anomalies in the eastern tropical Pacific and the convective activity anomaly in the western warm pool could affect the energy transfer between the tropics and the middle-high latitudes through the East-Asia–Pacific (EAP) teleconnection pattern (Gong et al. 2018). The energy transport mentioned above induces anomalies in atmospheric circulation at mid-to-high latitudes, which affects NECV and then the precipitation pattern in China (Nitta 1987; Nitta and Hu 1996; Zong et al. 2008; Sun et al. 2019; Wu et al. 2022; Zhang et al 2023). Aside from the influence of the tropical oceans, precipitation in the NEC region is also influenced by factors originating from the mid-to-high latitudes. It has been noted by M. Zhang et al. (2022a, b) that the SST variability in the North Atlantic contributes the out-of-phase change of precipitation in NEC from April to May.

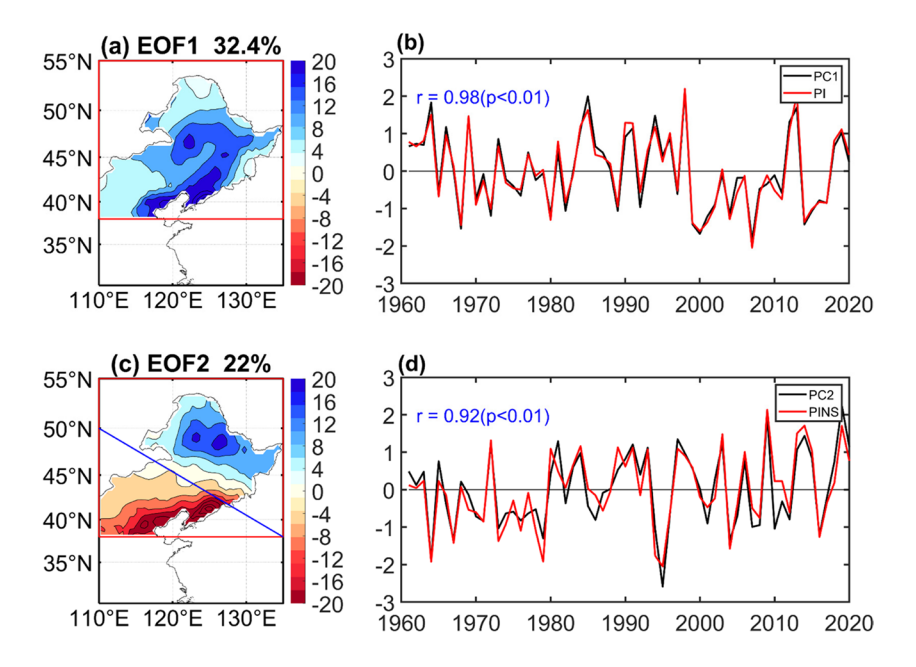
Previous research identified two major circulation patterns affecting summer precipitation in Northeast Asia: the Eurasian (EU) teleconnection propagated along the polar frontal jet (Wallace and Gutzler 1981), and the EAP teleconnection from low to high latitudes (Huang and Li 1988). These teleconnections serve as bridges between external forcing factors (e.g., SST/snow cover/sea ice) and East Asian climate (Li et al. 2022), with their spatial location and intensity changes significantly impacting the region. Arctic spring temperature increase and the corresponding change in spring sea ice are closely related to China's summer precipitation (Li and Leung 2013). Arctic sea ice anomalies in the spring can cause atmospheric circulation anomalies that persist into the summer, affecting summer wind circulation, water vapor transportation and thus precipitation in East Asia (Zhao et al. 2004; Guo et al. 2014). Furthermore, Zhang et al. (2019) have pointed out that the variability of Arctic sea ice interacts with Eurasian snow cover, where a decrease in Arctic sea ice can trigger teleconnection patterns in midto-high latitudes. However, such circulation anomalies lead to increased snow cover in these latitudes, resulting in temperature decreases. Moreover, the prolonged climatic effects of snow cover, through soil moisture anomalies, reduce incoming solar radiation, altering the heat/cold source forcing of East Asian summer climate, consequently inducing cold air masses and low-pressure systems over Northeast Asia (Zhao et al. 2004, 2024; Wu et al. 2009a, b; Honda et al. 2009). Therefore, the Eurasian spring snow cover also influences the summer precipitation in China (Lu et al. 2020; Zhang et al. 2016), by reducing solar radiation entering the surface due to high albedo, and then affecting large-scale circulation anomalies (Thackeray et al. 2019; Zhao et al. 2023). Additionally, soil moisture changes caused by snow melt affect energy balance, feeding back to the anomaly of large-scale circulation and then causing the summer rainfall patterns anomaly in East Asia. (Liu and Michio 2002; Xu and Dirmeyer 2011; Dirmeyer and Halder 2017; Zhang et al. 2017; Liu et al. 2017; Wang et al. 2024).

Ding et al. (2008) have pointed out the existence of a meridional dipole pattern in the distribution of summer precipitation in the East China region. However, most of these studies consider NEC as a whole, focusing primarily on the seasonal evolution characteristics or interannual and interdecadal variations of regional mean annual and summer precipitation in the whole NEC region. While the average annual and summer precipitation in the NEC area exhibits an insignificant increasing trend due to its interdecadal variability (Han et al. 2015; Li et al. 2018), it's worth noting that Han et al. (2019) identified two modes of interannual variability in midsummer precipitation in the NEC, with the maximum center of precipitation change located in either the southern or northern part of NEC. This discovery highlights the significant spatial heterogeneity in the precipitation distribution in the NEC, revealing the presence of a north-south opposite pattern of precipitation alongside the overall regional consistency (Han et al. 2021). Therefore, studying the spatial heterogeneity of summer precipitation in the NEC region will enhance our further understanding and prediction of interannual variations in summer precipitation in NEC. By no longer treating NEC as a whole but considering it in a more targeted manner, we can better prevent natural disasters caused by precipitation, ensuring the safety of people's lives and properties.

The summer precipitation in the NEC has shown opposite North–South patterns in the past 60 years (Fig. 1c), suggesting that the variation of precipitation in NEC has other spatial distribution characteristics beyond the overall consistency. Few studies have investigated the clear north–south opposite pattern of summer precipitation variations over NEC in recent decades and the mechanisms influencing them. The objective of this study is to examine the properties of north–south dipole precipitation patterns in the NEC region by addressing the following issues: 1) Is there an out-of-phase pattern



Fig. 1 The first leading mode of the EOF (a) and its normalized time series (black line) and PI (red line), and the second leading mode (c) and its normalized time series (black line) and PINS (red line) (d) of summer precipitation field in Northeast China during 1961–2020



of precipitation exist over the NEC region? 2) What causes the summer precipitation in NEC to show anomalous out-of-phase changes? Exploration these issues could deepen our scientific understanding of the variations of summer rainfall over the NEC and could also improve the summer dry—wet prediction and drought/flood mitigation.

### 2 Data and methods

The main datasets used in this study are monthly averages of air temperature, geopotential height (HGT), horizontal wind field (u and v), and omega from the NCEP/NCAR reanalysis data for the period 1961-2020. Daily precipitation observations from 2472 stations spanning from 1961 to 2020 were interpolated into  $0.5^{\circ} \times 0.5^{\circ}$  grid cells and converted into monthly scale data (Shen et al. 2010). We also used Mann Kendall non-parametric trend tests to analyze the data trends, and the data was sourced from the China Meteorological Administration (CMA). In addition, the monthly SST data, sea ice, snow depth (Varga and Breuer 2023; Akyurek et al. 2023; Mortimer et al. 2020; Yang et al. 2016), volumetric soil water layer 2 (7-28 cm)( Beck et al. 2021; Li et al. 2020a, b), surface albedo, surface heat flux (sensible heat flux and latent heat flux), and vertically integrated moisture divergence, vertical integral of northward and eastward water vapor fluxes and so on, from ECMWF Reanalysis v5 (ERA5) are also used in this study (Hersbach et al. 2020; Muñoz-Sabater et al. 2021).

The precipitation index in NEC (PI) is calculated from the regional average precipitation anomaly in NEC (38°N-55°N, 110 to 135°E). Here, the anomaly is based on the 1981–2010 mean. The average precipitation in the northern part of NEC (north of the blue line in Fig. 1c, the

range is:  $46 \sim 55^{\circ} N,117 \sim 135^{\circ} E$ ) minus that in the southern part (south of the blue line in Fig. 1c, the range is:  $38 \sim 46^{\circ} \text{N}, 110 \sim 128^{\circ} \text{E}$ ) is the NEC north-south opposite type precipitation index (PINS). Using a similar approach to Wallace and Gutzler (1981) and Wakabayashi and Kawamura (2004), combined with the actual research in this paper, we define the EU teleconotation index as follows:  $EUI = -\frac{1}{4}HGT'(55^{\circ}N, 20^{\circ}E) + \frac{1}{4}HGT'(55^{\circ}N, 75^{\circ}E) - \frac{1}{4}HGT'(40^{\circ}N, 145^{\circ}E)$ where HGT represent the normalized 500-hPa geopotential height at a given latitude and longitude. Similarly, the EAP teleconnection index is defined as: EAPI =  $-\frac{1}{4}$ HGT'<sub>s</sub>(60°N, 145°E) +  $\frac{1}{2}$ HGT'<sub>s</sub>(50°N, 120°E) -  $\frac{1}{4}$ HGT'<sub>s</sub>(25°N, 100°E) where  $HGT'_s = HGT' \sin 45^{\circ} / \sin \varphi$ ,  $\varphi$  is  $60^{\circ}N$ ,  $50^{\circ}N$ ,  $25^{\circ}N$ , respectively (Huang 2004; Choi et al. 2010). We also use the wave activity flux (WAF; Takaya and Nakamura 2001) to study and analyze the propagation characteristics of Rossby waves in the upper troposphere.

Other indices including the northeast China Low index (NECLI), is defined as the area-averaged HGT at 500-hPa level within  $40^{\circ}$ – $50^{\circ}$ N,  $120^{\circ}$ – $130^{\circ}$ E multiplied by –1 (Liu et al. 2012). Here, the larger the NECLI, the stronger the northeast China Low (NECL). An ENSO-like SST index (ENSSTI) is defined as the area averaged SST within 80°W to 150°W, 5°N to 5°S minus the area average within 120°E to 150°E, 20°N to 10°S. This definition is similar to Cao et al. (2013) and actually better presents the ENSOrelated seesaw pattern in SST anomaly over the tropical Pacific. The snow depth index (EBSDI) is defined as the area-averaged snow depth within 40°E to 60°E, 60°N to 70°N minus the area average within 100°E to 115°E, 50°N to 58°N. And the sea ice index (SICBKI), is defined as the area average within 35°E to 85°E, 74°N to 78°N. In this study, the data used for regression or correlation were de-trended. The correlation coefficients of all indices are shown in Table 1.



**Table 1** Correlation coefficient of each index (\* means pass 90% significance test, \*\* means pass 95% significance test)

		NECLI	EUI MAM JJA		EAPI MAM JJA		ENSSTI	EBSDI	SICBKI
PC2	,	0.45**	-0.16	0.04	0.08	-0.39**	0.26**	0.29**	0.34**
NECLI		\	-0.18	0.07	0.23*	-0.01	0.33**	0.42**	0.04
EUI	MAM	\	\		\		-0.06	-0.29**	-0.09
	JJA						0.28**	0.11	0.24*
EAPI	MAM	\	\		\		0.37**	0.14	0.16
	JJA						-0.25**	0.04	-0.12

#### 3 Results

# 3.1 South-North dipole in summer precipitation over NEC and its corresponding atmospheric circulation

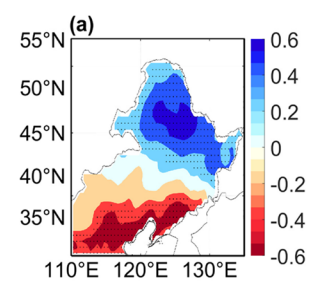
It is well-established that the majority of precipitation in NEC mainly occurs in summer (JJA), accounting for about 65% of the annual total (Liang et al. 2011). Therefore, our study will primarily focus on this season. However, in addition to the overall variations observed in precipitation in NEC, a north-south contrasting precipitation pattern is also evident (Fig. 1c), highlighting the significance of considering regional variability.

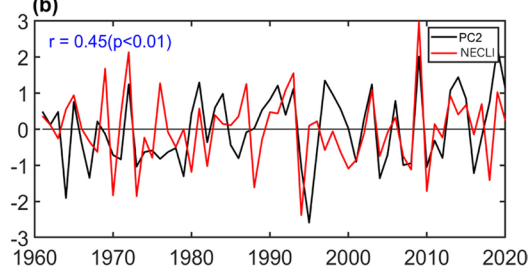
To identify the primary patterns of summer precipitation over NEC from 1961 to 2020, an EOF analysis was conducted. The first EOF mode, as shown in Fig. 1a, distinctly captures the one-sign changes in summer precipitation across NEC with an explained variance of 32.4%. The time series corresponding to the first mode (PC1, black line) correlates strongly with the area-averaged summer precipitation (PI, red line) in NEC (Fig. 1b), exhibiting a correlation coefficient of 0.98, significant at the 5% level. In the EOF2 mode, the summer precipitation variation in the NEC region shows a general northeast-southwest orientation, with high values located in both the northern and southern parts of NEC (Fig. 1c). Therefore, in this study, we refer to the precipitation pattern in NEC as the North-South Dipole Mode precipitation. The corresponding time series of EOF2 (PC2, black line) is significantly associated with the PINS index (red line), with a correlation coefficient of 0.92(Fig. 1d), reflecting the contrasting north–south precipitation pattern for the NEC region in summer.

From 1961 to 2020, opposite north-south type of precipitation occurs 24 times during the summers, accounting for about 40% of the total. However, this summer precipitation dipole has been largely overlooked in previous studies, which have either focused on regional changes considering NEC as a whole, or devoted to the meridional tripole and dipole precipitation structures in eastern China (Wang et al. 2020). Therefore, it is both essential and urgent to characterize and understand the causes of the north-south antiphase precipitation during summer in NEC. Subsequent research will rely on the PC2 index, which well represents the regional north-south precipitation dipole over NEC. A positive PC2 index signifies a south dry - north wet pattern in NEC, and vice versa (Fig. 2a). In addition, the correlation coefficient between PC2 and NECLI reaches 0.45 (passing the 99% significance test, Fig. 2b).

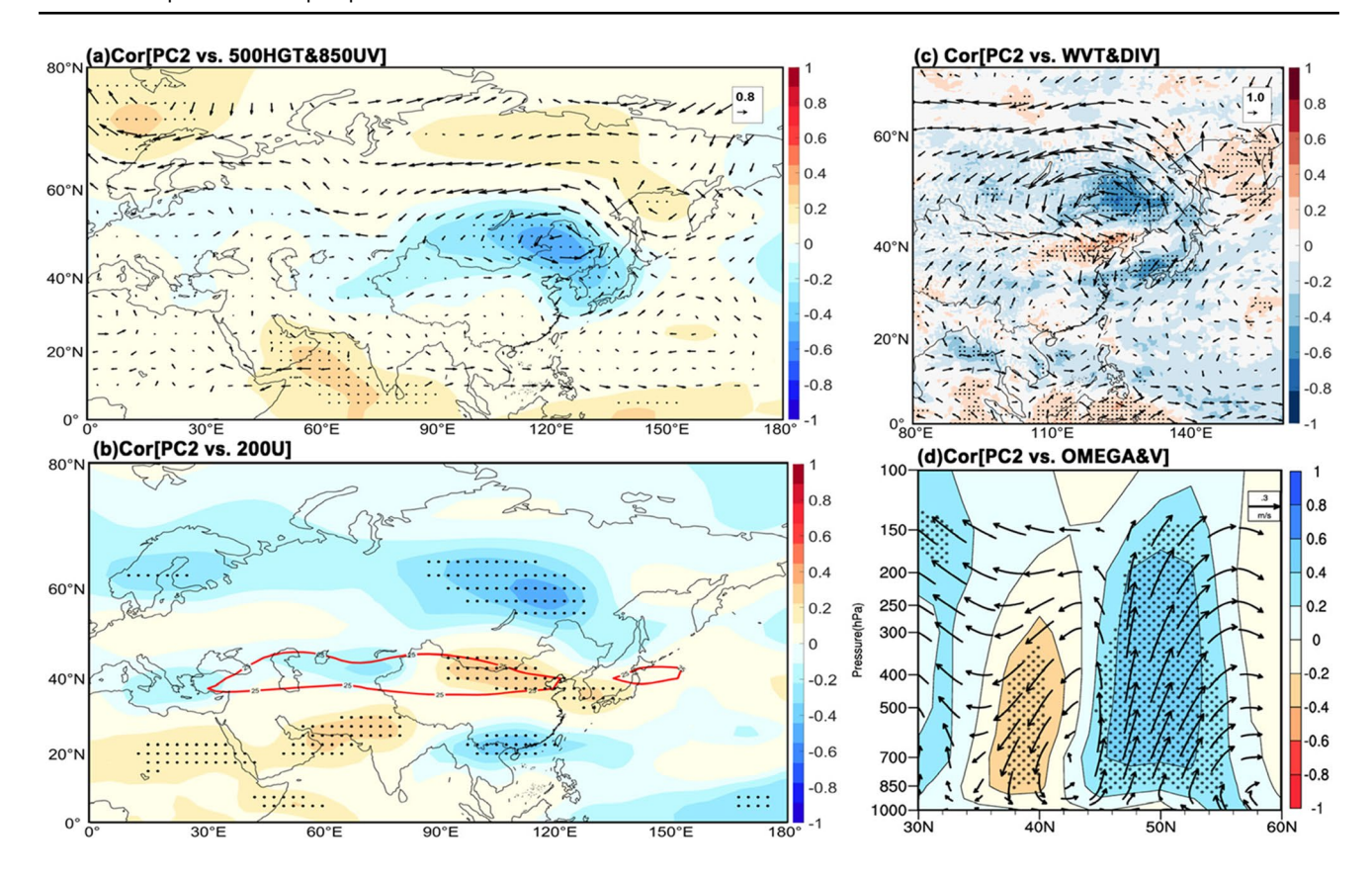
To investigate the out-of-phase change of summer precipitation in NEC, we analyze the accompanying anomalies in atmospheric circulation. As depicted in Fig. 3a, the correlation field in the 500-hPa HGT with PC2 shows that NEC is under the influence of an anomalously negative pressure center. The corresponding cyclonic wind field at 850-hPa reveals moist southeasterly winds in the north and dry westerly winds in the south of the NEC. The anomalous southeasterly winds thereby transport more water vapor from the North Pacific Ocean to the northern NEC (Fig. 3b, c). The anomalous westerlies in the southern NEC enhance the East Asian subtropical

Fig. 2 Correlation coefficients between PC2 and summer precipitation in NEC (a), and (b) the normalized time series of NECLI (red line) and PC2 (black line) for 1961–2020. The NECLI values are multiplied by – 1. Regions above the 95% significance level are dotted









**Fig. 3** Correlation coefficients of 500-hPa HGT (**a**, shading) and 850-hPa horizontal wind vector (**a**, vectors), 200-hPa U-wind (**b**, shading), water vapor flux (**c**, vectors) and divergence (**c**, shading) in summer with PC2 during 1961–2020. Latitude–height cross section of regressed meridional wind (vectors; m s<sup>-1</sup>) and vertical velocity

(shading, unit:  $10^{-2}$  Pa s<sup>-1</sup>) along  $110^{\circ}$ – $135^{\circ}$ E in summer against PC2 (**d**) during 1961–2020. The Omega values are multiplied by –100. The red line in b is the climatic westerly jet. Regions at the significance level of 5% are dotted

westerly jet around the 40°N. This, in turn, promotes downward motion below the jet primarily through the poleward advection of warm air. The advection of warm air warms the upper troposphere and suppresses convection (Lu et al. 2007). Additionally, the enhanced jet stream leads to an increased horizontal temperature gradient, resulting in stronger vertical wind shear, which further contributes to enhanced subsidence beneath the jet (Du et al. 2022a, b). In addition, an abnormal updraft and an anomalous convergence of water vapor flux in the northern part of NEC, coupled with the anomalous descending motions and water vapor flux divergence in the southern part of NEC (in Fig. 3d), align with the observed patterns of increased precipitation in the north and decreased precipitation in the south (Fig. 1c).

Previous studies have explored the impacts of the Northeast China Vortex (NECV) on climate conditions, and the occurrence of NECV has been found conductive to the formation of precipitation in NEC (Liu et al. 2002; Hu et al. 2011; He et al. 2007). Given our findings of a significant low-pressure center over NEC and its associated circulations being favorable to the precipitation dipole over the NEC, we

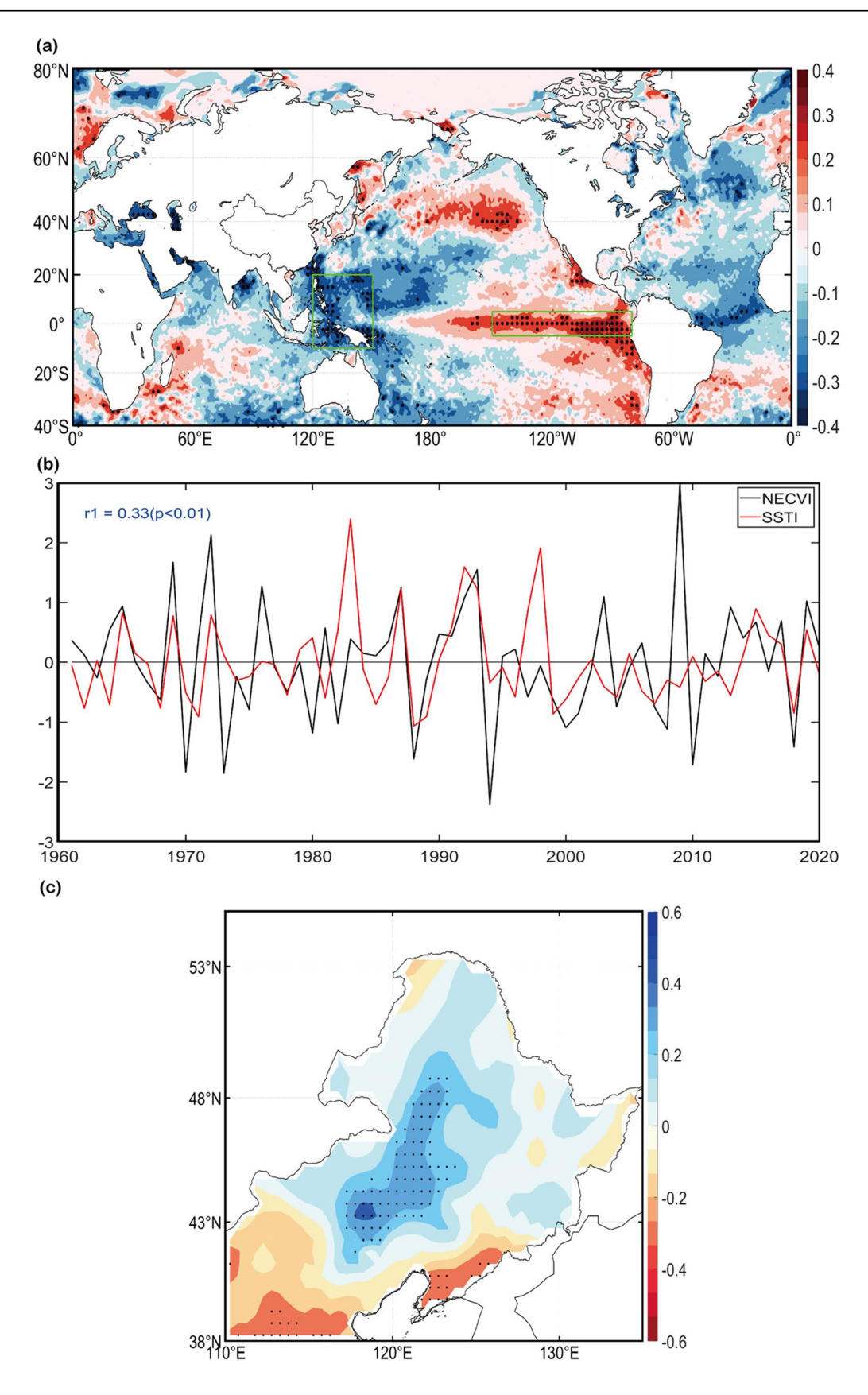
define the NECLI to describe precipitation over the NEC (Du et al. 2016). The results show a good correlation with PC2 time series, with the correlation coefficient of 0.45 at the significance level of 5% (in Fig. 2b). This indicated that the stronger the northeastern low pressure, the more pronounced the summer precipitation dipole over NEC, with increased precipitation in the north and decreased precipitation in the south (Fig. 2a).

## 3.2 Possible Mechanism of the summer precipitation dipole over Northeast China

### 3.2.1 Possible physical mechanisms in the perspective of SST

Since SST variability can cause atmospheric circulation anomalies near the equator and the subtropical zone, it can affect the climate in the mid-high latitudes through the teleconnection between the instantaneous season and the subsequent season (Han et al. 2017; Wang et al. 2013; Choi and Ahn 2019; Wang et al. 2000), we therefore analyzed the relationship between summer precipitation in NEC and







**√Fig. 4** The correlation between summer NECLI and pre-spring SST (a), (b) the time series of NECLI (black line) and SST index (red line), and (c) correlation distribution of ENSSTI with precipitation in NEC. The green box is the key SST area. Regions at the significance level of 5% are dotted

preceding spring SST. Our results demonstrate a significant positive correlation between summer NECLI and spring SST in the tropical eastern Pacific, while it is negatively correlated with the western Pacific warm pool (Fig. 3a). Considering this ENSO-like SST pattern as a whole, we defined an ENSSTI index as the area-averaged differences of SST between the east and west equatorial Pacific, which shows a high correlation with the NECLI in the following summer, with a correlation coefficient of 0.33 at a 0.05 level of significance (Fig. 3b). The ENSSTI effectively captures the north—south wet-dry precipitation pattern (Fig. 3c) in NEC.

The associated circulation field suggests that an ENSO-like SST pattern in the tropical Pacific stimulate meridional "-+-" and zonal "+--+" atmospheric circulation anomalies.

Positive geopotential height anomalies are observed over the West Siberian Plain, the Kazakh Uplands, and south of the Sea of Japan toward the Philippines, resulting in a low pressure anomaly over the East European Plain and extending from NEC to the adjacent North Pacific (Fig. 4a). In the northern subregion of the Northeast Pacific, the advection of warm and humid air from the North Pacific, coupled with ascending motion, facilitates an increase in precipitation. Conversely, the southern subregion exhibits contrasting characteristics, with a decrease in precipitation (Fig. 4b-d). Thus, we conclude that the spring equatorial Pacific SST has a significant influence on anomalous NECL and thus the summer precipitation dipole in NEC by triggering the EU and EAP teleconnections. The dipole precipitation pattern in NEC exhibits a positive correlation with springtime SSTs in the eastern tropical Pacific and a negative correlation with SSTs in the western region. This indicates that the generation of ascending motion occurs in the eastern region, which weakens the Walker circulation near the equator and induces descending motion in the western region,

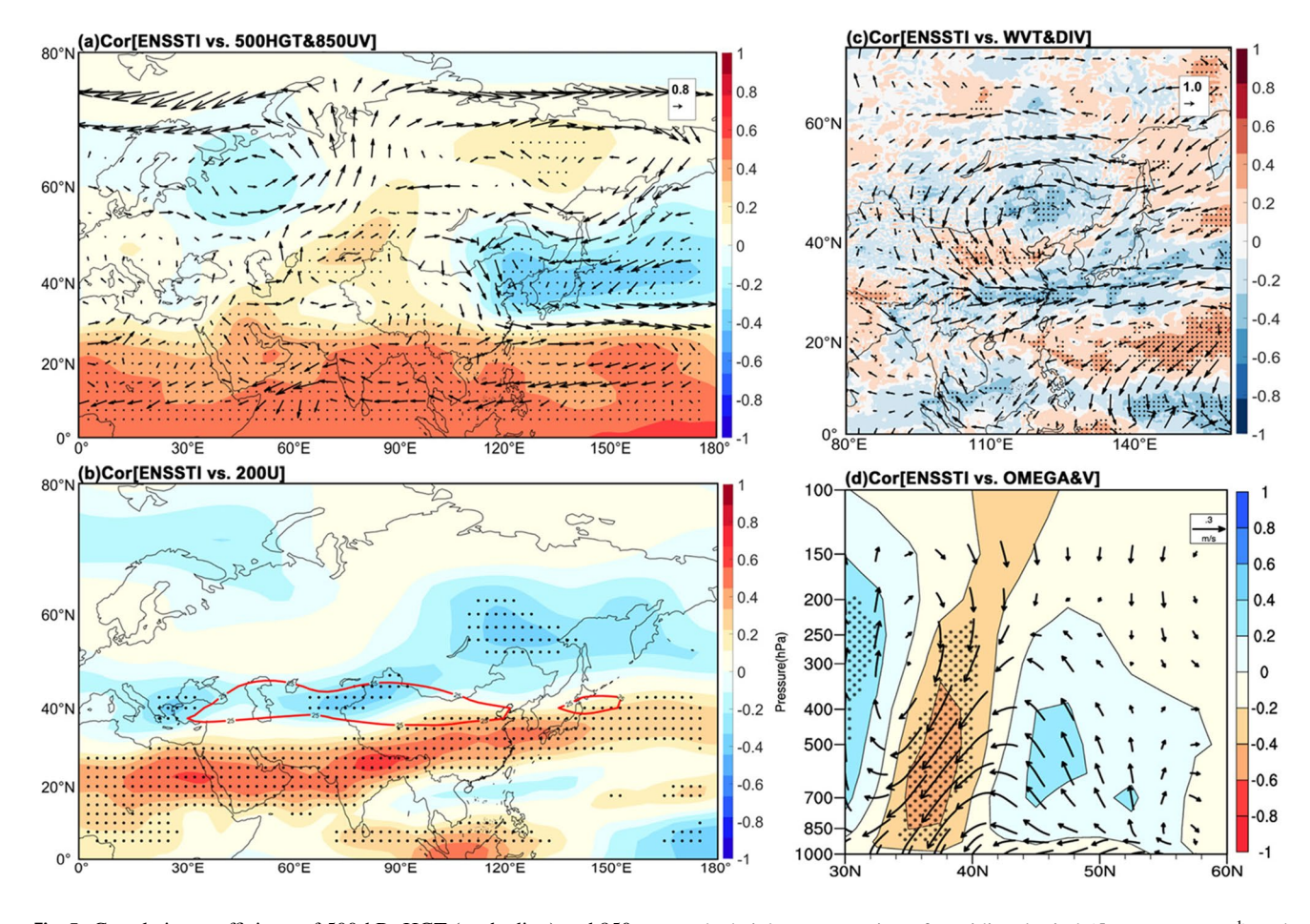


**Fig. 5** Correlation coefficients of 500-hPa HGT (**a**, shading) and 850-hPa horizontal wind vector (**a**, vectors), 200-hPa U-wind (**b**, the red contour is the climatic westerlies), water vapor flux (**c**, vectors) and divergence (**c**, shading) with the ENSSTI. Regressions of the lati-

tude-height cross section of meridional wind ( $\mathbf{d}$ , vectors; m s<sup>-1</sup>) and vertical velocity ( $\mathbf{d}$ , shading:  $10^{-2}$  Pa s<sup>-1</sup>) along  $110^{\circ}$ – $135^{\circ}$ E in summer with the ENSSTI during 1961–2020, the Omega values are multiplied by – 100. Regions at the significance level of 5% are dotted



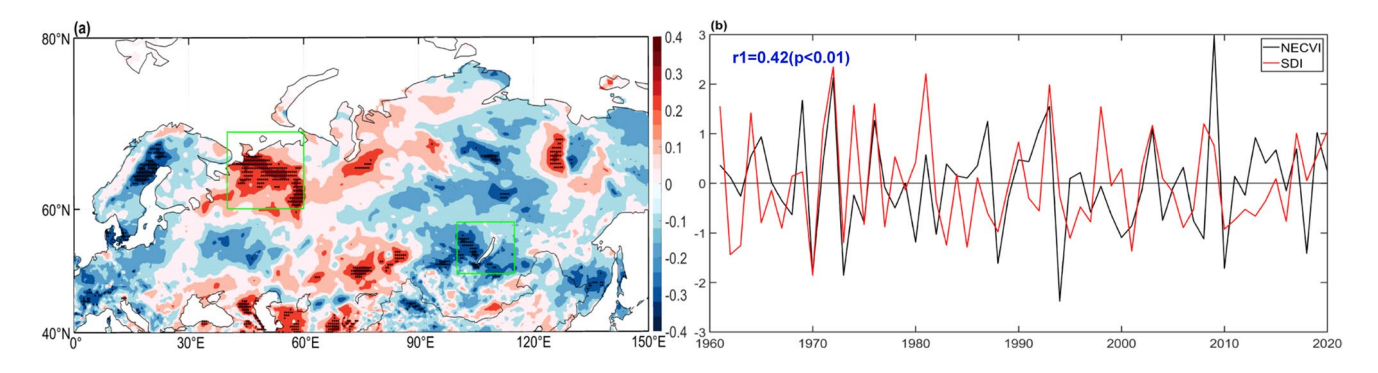
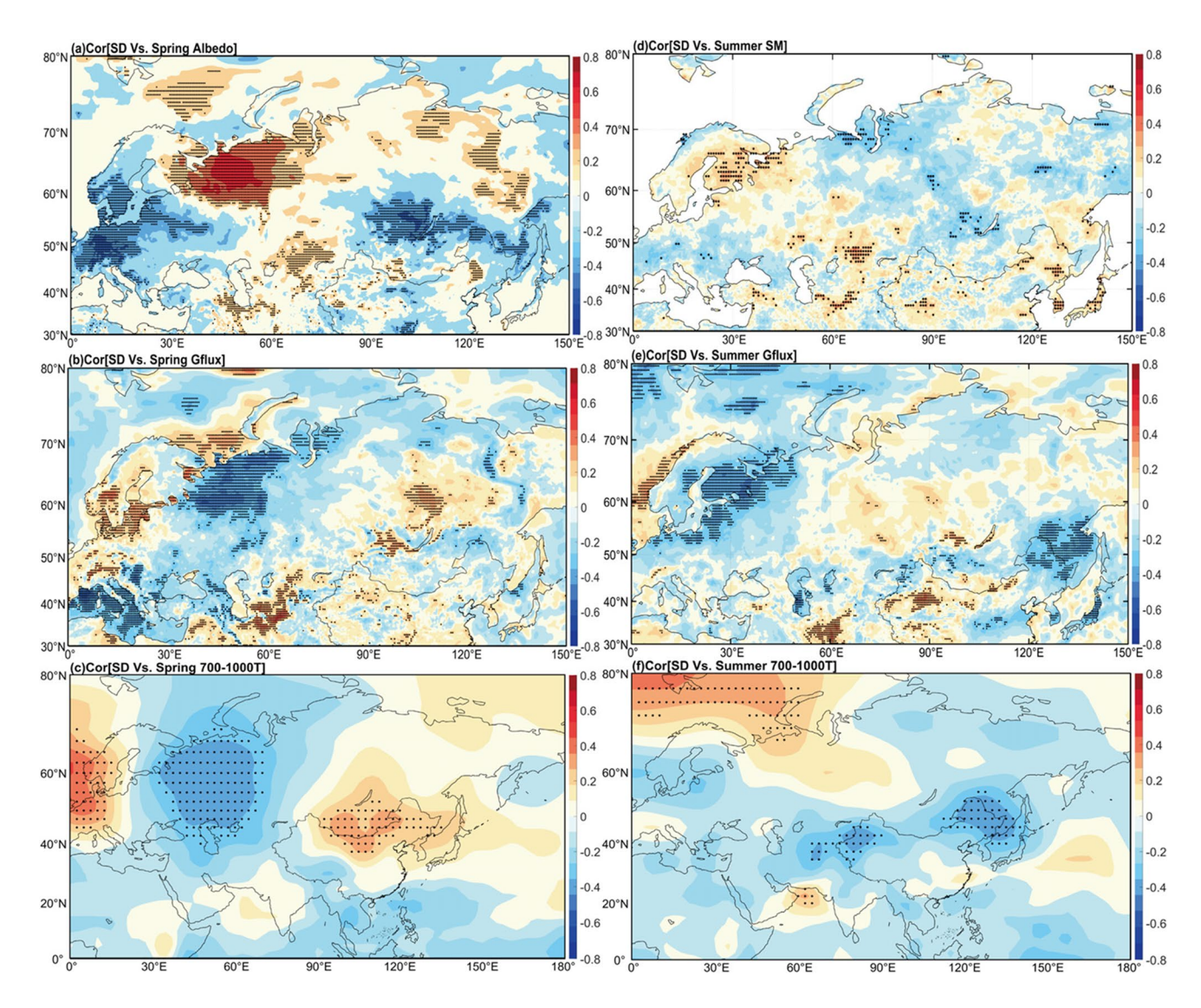


Fig. 6 The correlation between summer NECLI and pre-spring snow depth (a), and (b) the time series of NECLI (black line) and SD index (red line). The green box is the key SD area. Regions at the significance level of 5% are dotted



**Fig. 7** The correlation between spring EBSDI and spring albedo (**a**), surface heat flux (**b**) and lower atmosphere temperature, and atmospheric thickness between 700-hPa and 1000-hPa (**c**), as well as the

correlation distribution of summer soil moisture (d), surface heat flux (e) and atmospheric thickness between 700-hPa and 1000-hPa (f). Regions at the significance level of 5% are dotted



consequently suppressing convective activity in the Philippines region (Wu et al. 2017; Pierrehumbert 2000; Dang et al. 2020; McPhaden et al. 2006; Wang et al. 2000). As a result, a meridional teleconnection pattern is similar to the EAP pattern is triggered, leading to the occurrence of negative anomalies in geopotential height over the NEC to Pacific region (Lu et al. 2006; Huang and Li 1988). Indeed, the zonal wind pattern in summer involved with spring ENS-STI displays a similar EAP-pattern with those in Fig. 5b with NEC precipitation dipole. The correlation between the ENSSTI and EAPI is -0.25 which is significant at 5% level (see Table 1).

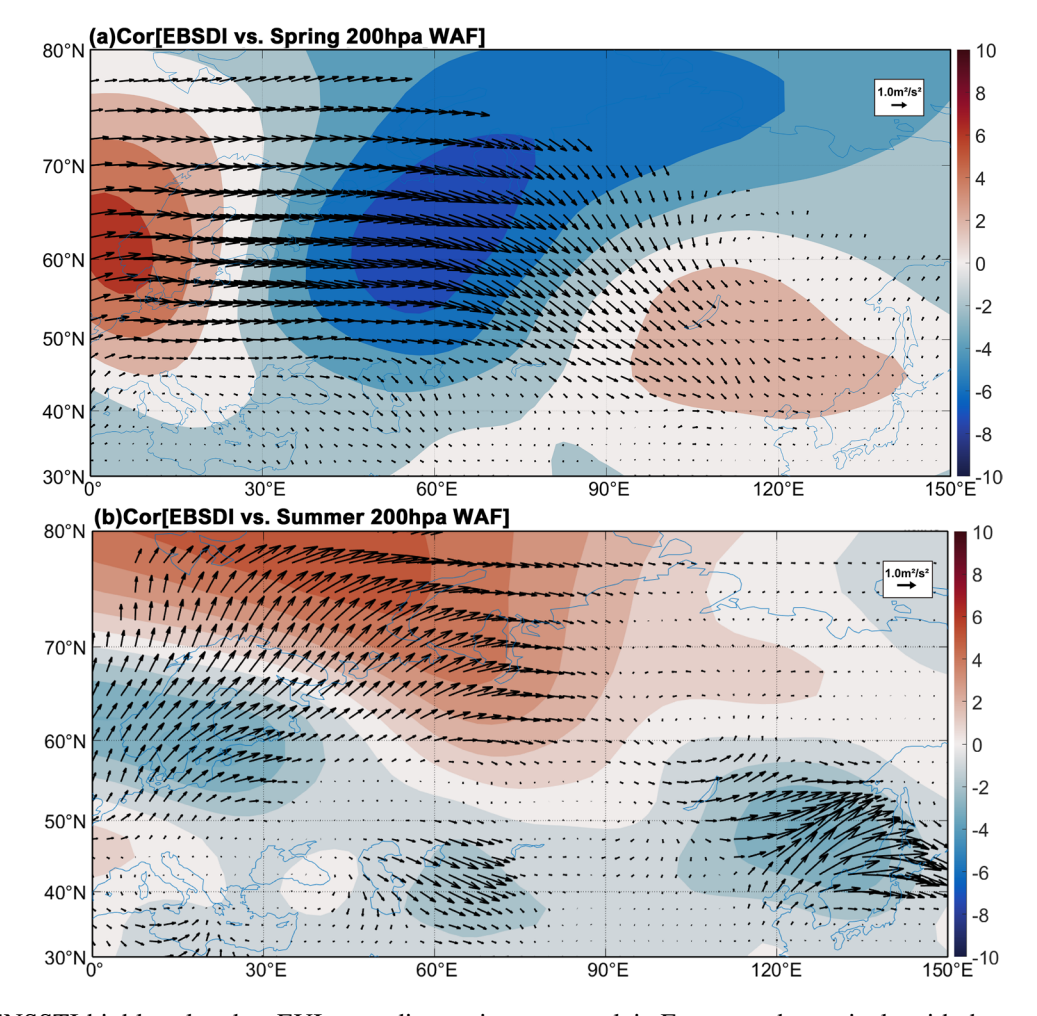
Furthermore, previous research has demonstrated that SST anomalies resembling the ENSO can initiate the distant EU teleconnection pattern, which propagates along the subtropical jet stream in the mid-high latitude region (Sun et al. 2021a, b; Wu and Wang 2002). This propagation can occur through the transmission of Rossby wave rays into the Atlantic region or via the teleconnection pattern associated with the Arctic Oscillation (Feng et al. 2017; Hu et al.

in the succeeding summer, with a correlation coefficient of 0.28 at a 5% significant level (Table 1). Therefore, the latitudinal EU teleconnection maintained in the mid-high latitudes related to the ENSO-like pattern of SST in the tropical Pacific Ocean is conducive to maintaining an anomalous low pressure over NEC (Hu et al. 2020) and thus altering the precipitation dipole in this region in summer.

### 3.2.2 Possible physical mechanisms in the perspective of Eurasian snow cover

Variations in winter and spring snow cover across Eurasia also significantly impact the East Asian climate by modulating the proportion of solar radiation absorbed and creating persistent soil moisture anomalies (Lu et al. 2020; Zhang et al. 2016). As illustrated in Fig. 6a, our analysis identified the spring snowpack in Europe and the vicinity of Lake Baikal as pivotal in influencing the NECL, which in turn affects the summer precipitation dipole in the NEC region. Notably, the NECLI correlates positively with pre-

**Fig. 8** Horizontal wave activity flux (vector,m<sup>2</sup>s<sup>-2</sup>) at 200-hPa and HGT anomalies (shading, gpm) at 200-hPa in (**a**) spring and (**b**) summer in association with the spring EBSDI during 1961–2020



2018). Statistically, spring ENSSTI highly related to EUI

ceding spring snowpack in Europe and negatively with that



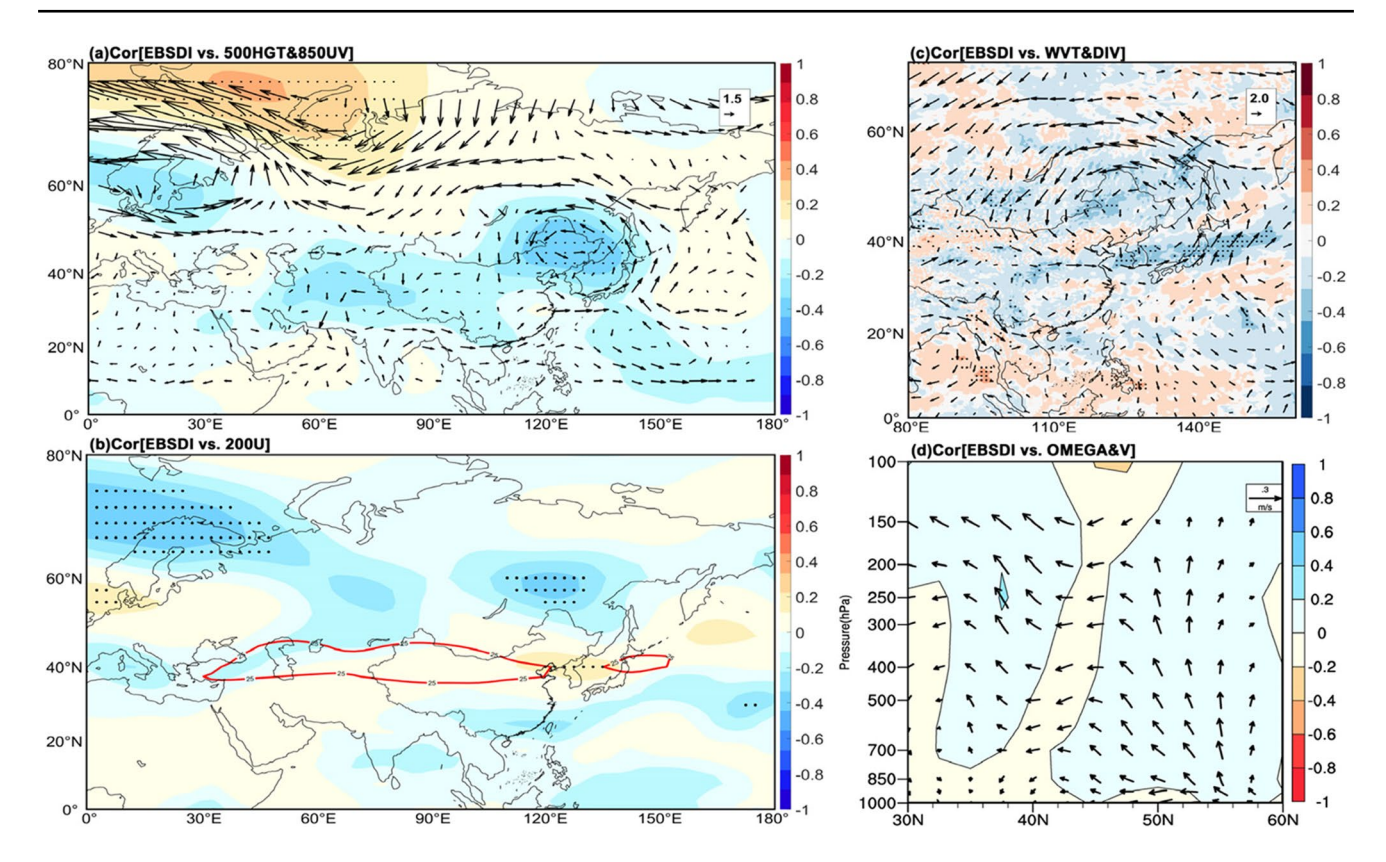


**Fig. 9** Correlation coefficients of 500-hPa HGT (**a**, shading) and 850-hPa horizontal wind vector (**a**, vectors), 200-hPa U-wind (**b**, the red line is the climatic westerlies), water vapor flux (**c**, vectors) and divergence (**c**, shading) with the EBSDI. Regressions of the latitude—

height cross section of meridional wind ( $\mathbf{d}$ , vectors; m s<sup>-1</sup>) and vertical velocity ( $\mathbf{d}$ , shading:  $10^{-2}$  Pa s<sup>-1</sup>) along  $110^{\circ}$ – $135^{\circ}$ E in summer with the EBSDI during 1961–2020, the Omega values are multiplied by – 100. Regions above the 5% significance level are dotted

near Lake Baikal. The combined effects of snow cover in these two regions influence the dipole pattern of summer precipitation in NEC (Zhang et al. 2021a, b; Liu and Yanai 2002; Jia et al. 2018). The correlation has statistical significance, with the correlation coefficient of 0.42 at a significance level of 0.01 (Table 1; Fig. 6b).

The dynamics of this relationship are elucidated in Fig. 7. As explained by Cohen and Rind (1991), the increase in snow cover during the previous spring led to an increase in surface albedo, which in turn reduced the absorption of shortwave radiation and the upward surface heat flux. This, in turn, initiates circulation anomalies downstream from regions with anomalous heat sources (Fig. 7a, b).

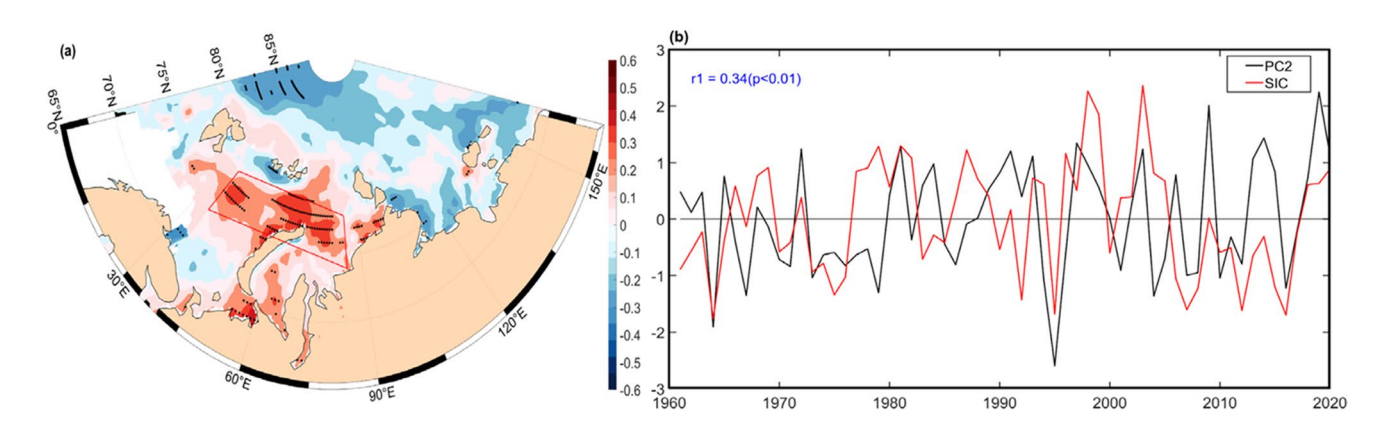


Fig. 10 The correlation between summer PC2 and pre-spring sea-ice cover (a), and (b) the time series of PC2(black line) and SIC index (red line). The red box is the key SIC area. Regions above the 95% significance level are dotted



Furthermore, the increased snow in Europe is often accompanied by more sea ice over the Barents Sea and its surrounding waters, which has a high albedo and acts as a cooling mechanism. In Fig. 7c, the lower tropospheric (700–1000 hPa) atmospheric thickness anomalies corresponding to EBSDI are depicted. A notable thinning of the atmosphere over Europe and a thickening over the area east of Lake Baikal are observed. During the spring season, the anomalous upper tropospheric WAF triggers the propagation of Rossby waves across Eurasia. This process generates a distinct pattern of geopotential height anomalies that spans from the Arctic to East Asia. The pattern exhibits a quasibarotropic structure resembling a configuration of "+—+" anomalies (Fig. 8a). This results in a positive pressure anomaly over Northeast Asia.

The influence of increased or decreased EBSDI in spring can persist into the summer months (Li et al. 2018; Zhang S et al. 2022a). Research has shown that spring snow cover can

have a significant impact on subsequent summer precipitation and temperature through hydrological effects (Xu et al. 2021). As the excessive snow in Europe melts during the following summer, it increases soil moisture, thereby reducing the surface heat flux and causing cooling in the lower atmosphere (Fig. 7d, e, f). Anomalous soil moisture can affect the abnormal heating/cooling of the atmosphere, leading to anomalous thickness in the lower atmosphere (not shown in the figure), resulting in significant negative geopotential height anomalies over Eastern Europe and Northeast Asia (Fig. 9a) (Sun et al. 2021a, b; Liu et al. 2016).

During the summer, the perturbations in the upper troposphere, marked by a WAF anomaly, initiate a Rossby wave train that emanates from Europe, traverses the Arctic, and extends downstream to Northeast Asia. This dynamic process culminates in a reduced geopotential height over the NEC region, as shown in Fig. 8b. Moreover, the combination of enhanced snow cover in Europe and higher moisture

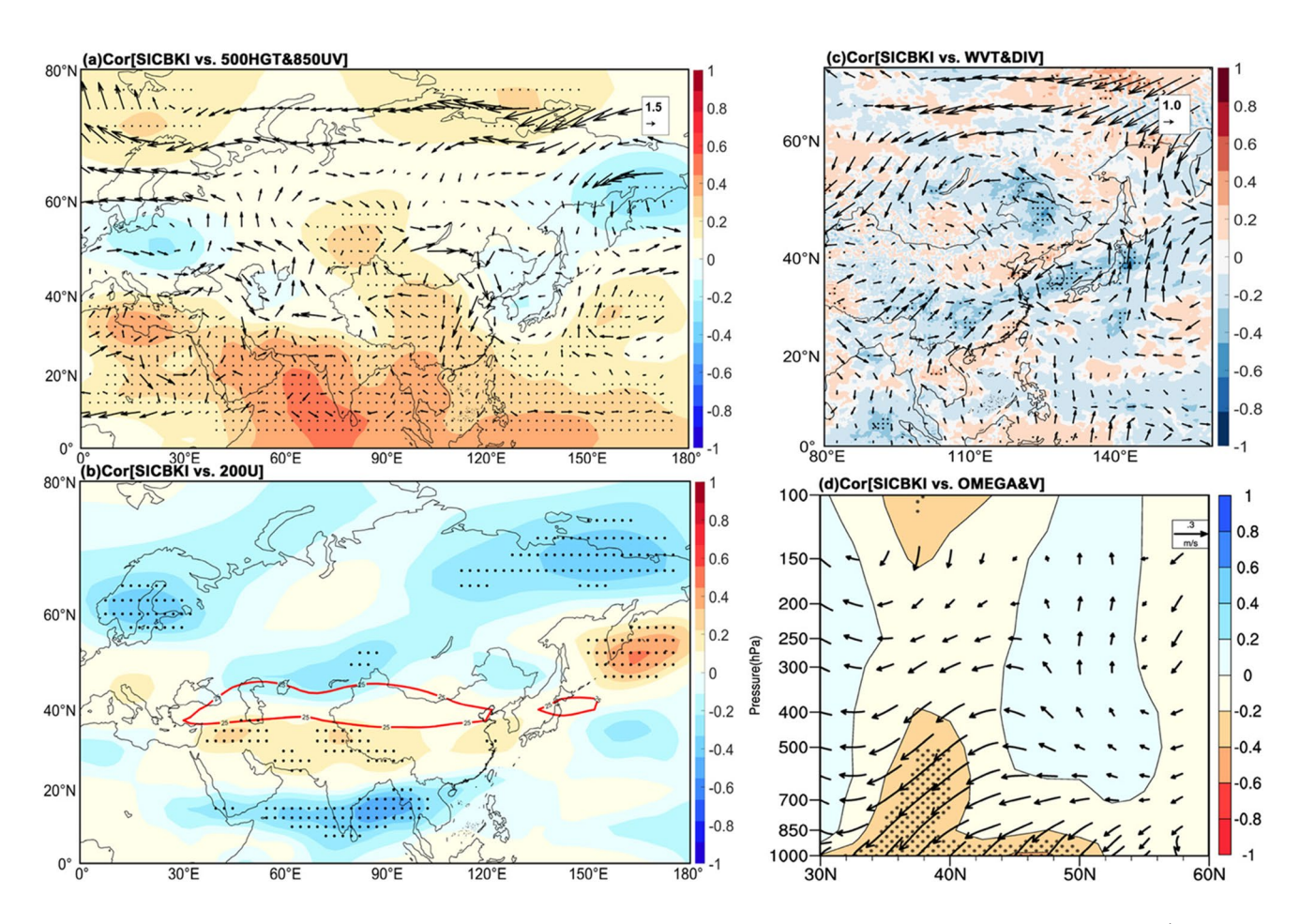


**Fig. 11** Correlation coefficients of 500-hPa HGT (**a**, shading) and 850-hPa horizontal wind vector (**a**, vectors), 200-hPa U-wind (**b**, the red line is the climatic westerlies), water vapor flux (**c**, vectors) and divergence (**c**, shading) with the SICBKI. Regressions of the latitude—

height cross section of meridional wind ( $\mathbf{d}$ , vectors; m s<sup>-1</sup>) and vertical velocity ( $\mathbf{d}$ , shading:  $10^{-2}$  Pa s<sup>-1</sup>) along  $110^{\circ}$ – $135^{\circ}$ E in summer with the SICBKI during 1961–2020, the Omega values are multiplied by – 100. Regions above the 95% significance level are dotted



levels during summer can influence atmospheric circulations, which may lead to increased precipitation over the Yangtze River valley and northern China. This is in line with the findings of Zuo et al. (2012). The resulting anomalous cyclone, together with contrasting water vapor fluxes and vertical movements over the NEC (Fig. 9), results in the formation of a dipole pattern of summer precipitation in the NEC.

### 3.2.3 Possible physical mechanisms in the perspective of Arctic sea ice

In addition to the Eurasian snow cover, many researches have elucidated the significant role of Arctic sea ice in shaping the climate of China and East Asia (Wu et al. 2009a, b; Han et al. 2021). Our findings reveal a significant positive correlation between spring sea ice and NEC summer precipitation dipole patterns in the regions north of the Barents Sea and Kara Sea, with a correlation coefficient (SICBKI and PC2) reaches 0.34 at the significant level of 5% (Fig. 10). This correlation underscores the influence of Barents-Kara sea ice in spring on the subsequent summer precipitation dipole pattern in NEC. Previous studies have identified the effects of Barents-Kara sea ice anomalies on atmospheric circulation and climate in East Asia through diagnostic

simulations of global atmospheric teleconnection patterns (Xie and Huang 1990; Petoukhov and Semenov. 2010).

Our study further delved into the changes in summer atmospheric circulation and find that the pre-spring Barents-Kara region sea ice has a certain influence on it, as shown in Fig. 11. An above-normal sea ice extent in the Barents-Kara Sea during spring initiates a "-+-" zonal wave train across the middle-high latitudes of Eurasia in summer, with a notable negative geopotential height anomaly positioned over the Sea of Okhotsk extending to NEC (Fig. 11a). This anomaly induces cyclonic circulation patterns in the northeastern region, resulting in the northern part being influenced by moist easterly winds from the sea, while the southern part is affected by dry westerly winds. The presence of a positive anomaly in the westerlies in the southern region (Fig. 11b), accompanied by significant subsidence, can lead to a reduction in precipitation, aligning with findings from previous research (Wu et al. 2009a, b; Wu et al. 2011). Consequently, the anomalous moisture convergence and upward motion are prevalent in the northern NEC, while the opposite condition are observed in the southern NEC (Fig. 11c, d), promoting precipitation in the north and suppression in the south.

Spring sea ice near the Barents-Kara Sea similarly reduces lower atmospheric temperatures by affecting albedo and surface heat flux (Fig. 12a-c). This triggers a Rossby wave teleconnection pattern across the middle and high

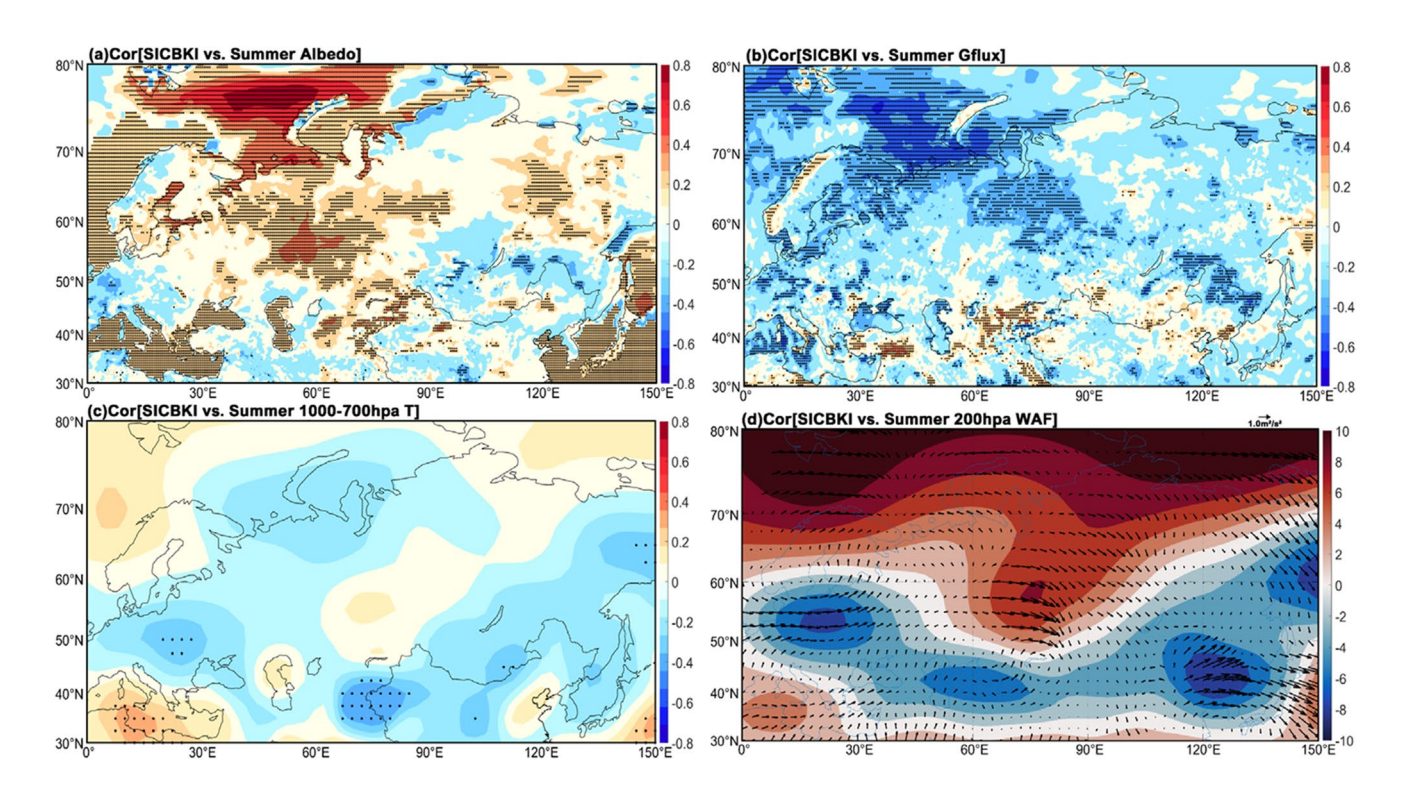


**Fig. 12** The correlation between spring albedo (**a**), surface heat flux (**b**) and lower atmosphere temperature (**c**, 700-1000hpa average atmospheric temperature) with the spring SICBKI, as well as the

regression distribution of summer 200hpa HGT (shading, gpm) and wave flux (vector, $m^2s^{-2}$ ) (**d**) in association with the spring SICBKI. Regions at the significance level of 5% are dotted



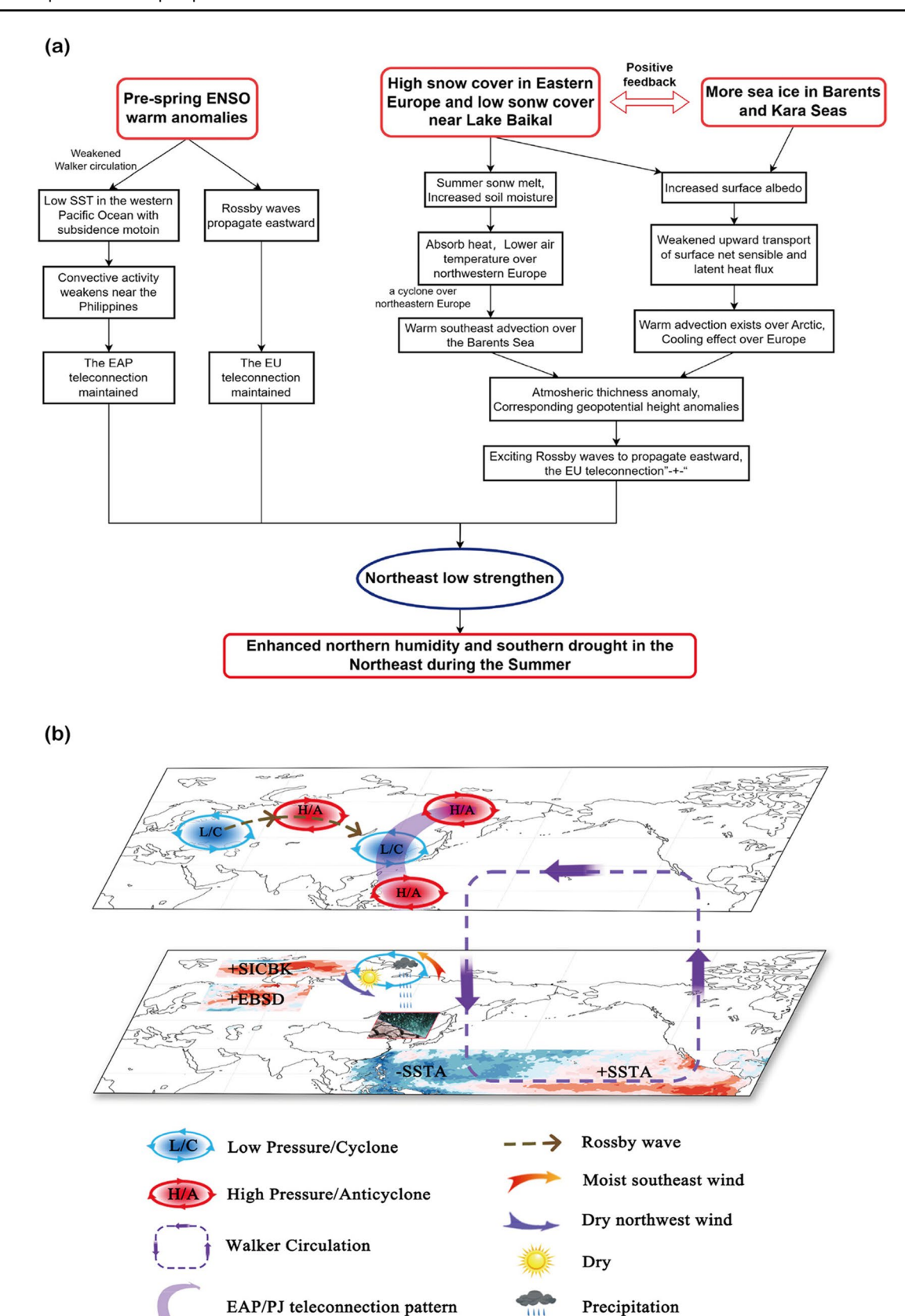


Fig. 13 The physical mechanism chain (a) and schematic diagram (b) of the dipole pattern of summer precipitation in the NEC



latitudes of Eurasia. During the summer, the zonal wave train linked to the Barents-Kara Sea ice in spring intensifies over the Eurasian sector (Fig. 12d). This wave train extends from the Atlantic to Northeast Asia, leading to negative height anomalies (indicating cyclonic circulation anomalies) over the NEC region. These anomalies contribute to the observed dipole pattern enhancement of summer precipitation in the NEC region.

The chain of mechanisms linking spring Barents-Kara sea ice to summer precipitation dipole in NEC bears resemblance to the influence of Eurasia spring snow cover. Prior studies have suggested a close interconnection between Barents-Kara sea ice and the depth and cover of snow (Li and Wang 2013; Li et al. 2018). An increase in Barents-Kara sea ice is associated with increased snow in Europe and decreased snow around Lake Baikal (figure not shown), as corroborated by Li et al. (2018). Wu and Kirtman (2007) point out that this pattern plays a crucial role in shaping a zonal dipole distribution, which has substantial implications for climate variability and change in China (Wu et al. 2014; Zhang et al. 2016).

### 4 Conclusions and discussions

In this investigation, we elucidate the interannual variability characteristics of the dipole precipitation pattern during the summer months in NEC spanning the years 1961 to 2020. Furthermore, we delve into the potential influencing factors and associated mechanisms. The EOF2 spatial pattern across the entirety of the NEC displays a distinct dipole distribution between the north and south. The PC2 associated with this pattern exhibits significant interannual variability. Our results suggest that the preceding spring's tropical SST, Eurasian snow cover, and Barents-Kara sea ice all contribute to enhancing the low-pressure system over the NEC. This enhancement occurs through various teleconnection patterns and atmospheric circulation dynamics, which subsequently influence the dipole precipitation pattern in the NEC. The previous spring equatorial Pacific SST triggered EU and EAP teleconnection patterns by influencing vertical motion and convective activity. The synergistic effect of these teleconnections increases precipitation in the northern NEC, while inducing an inverse effect in the southern region, aligning with the findings of Hu et al. (2020).

Our study reveals that the mechanisms by which snow cover and sea ice influence precipitation in NEC bear similarities. Prior researches have demonstrated a significant correlation between the sea ice in the Barents-Kara Sea and the extent of snow cover in northern Eurasia (Li and Wang 2013; Li et al. 2018). The increase in sea ice in the Barents-Kara Sea and snow cover in Europe can both enhance

surface albedo, reduce the upward heat flux from the surface, and excite eastward-propagating Rossby waves in the mid-high latitudes of Eurasia. This leads to the formation of anomalous low pressure and cyclonic centers over the northeast, resulting in abnormally humid easterly winds and generally dry westerly winds in the northern regions. This dynamic ultimately fosters a spatial distribution of summer rainfall in the NEC that is characterized by a higher volume in the north and a decrease in the south. The specific physical mechanism is illustrated in Fig. 13.

The dipole distribution of precipitation in NEC is undoubtedly a result of several interconnected factors. This analysis, however, is focused on determining the factors influencing the interannual variability of summer precipitation dipole in the NEC from 1961 to 2020. In addition to the three factors examined in this study, the higher soil moisture in the Yangtze River basin and North China during spring leads to increased precipitation in NEC (Zuo and Zhang 2007, 2016). The Anomalies in the Indian Ocean basin during spring affect the vertical motion over tropical and subtropical regions, thereby impacting the interannual variability of late summer precipitation in NEC (Zhao et al. 2019). Moreover, the Atlantic Multidecadal Oscillation and Pacific Decadal Oscillation also influence summer precipitation in NEC (Si et al. 2021; Liu et al. 2023). It is noteworthy that the Arctic sea ice has been decreasing on decadal scales, leading to reduced precipitation and exacerbated drought in the NEC (Du et al. 2022a, b). Additionally, Li et al. (2018) found an enhanced correlation between the Barents Sea ice and precipitation in the Northeast region after 1996/97. Therefore, future studies investigating the impact of Arctic sea ice on NEC precipitation should also consider the decadal relationship between the two factors. Furthermore, since the late 1990s, relationships similar to ENSO between SST and subsequent summer East Asian-Pacific (EAP) teleconnections have gradually weakened (Wang et al. 2023), while significant decadal variations have been observed between early spring tropical Pacific temperatures and summer precipitation in the NEC region (Han et al.2017). Moreover, there have been two decadal variations in Eurasian spring snowmelt patterns since the late 1970s and mid-2000s, with a closely linked Eurasian snowmelt dipole pattern and precipitation in the Northeast region (Cheng et al. 2022). These insights suggest that when studying the mechanisms influencing NEC precipitation, the role of these influencing factors on decadal timescales should also be considered. As global temperatures gradually rise in the future, Tabari (2020) predict that precipitation in the Northeast region will exhibit an increasing trend by the end of the 21st century. The spatiotemporal uneven distribution of precipitation may exacerbate the risk of droughts and floods. The dipole precipitation pattern in the Northeast region might contribute to the increasing trend in summer



precipitation in the NEC. Anomalous East Asian summer precipitation could lead to flood and drought disasters, posing significant risks and losses to human life, property, and the socio-economic fabric (Torti 2012; Zhang and Zhou 2015). Therefore, exploring the changing characteristics and causal factors of the dipole pattern of summer precipitation in the NEC plays a crucial role in enhancing predictions of NEC precipitation and disaster prevention and mitigation efforts. Moreover, while this study's conclusions are primarily grounded in observational and statistical analysis, it is essential to conduct numerical experiments to validate the proposed physical mechanisms in future work.

Acknowledgements This work was jointly supported by the National Science Foundation of China (41991231, 42075018), Foundation of Gansu Science and Technology Department (21JR7RA529) and Young Elite Scientists Sponsorship Program by CAST (GXH20220530-09).

Author's contribution Xinya Shu, Shanshan Wang: Conceptualization, Methodology, Writing- Original draft preparation, Writing- Reviewing and Editing. Hao Wang: Software, Data curation. Yuanyuan Hu, Yiwei Pang: Visualization, Investigation. Jianping Huang: Supervision, Validation.

Funding The authors have not disclosed any funding.

Data availability ERA5 reanalysis data are available from https://cds.climate.copernicus.eu/cdsapp#!/dataset/reanalysis-era5-single-levels-monthly-means?tab=form. The NCEP-NCAR reanalysis dataset is available at https://psl.noaa.gov/data/reanalysis/reanalysis.shtml. The observed precipitation data provided by the China Meteorological Agency: http://data.cma.cn/. Due to the data policy in China, these data records are currently not available via a website for public download. However, researchers could contact the China Meteorological Data Service Center (http://www.cma.gov.cn/en2014/aboutcma/contactus/) for detailed information on data acquisition. Figures in this manuscript were made with MATLAB version 2020a and this software is available from www.mathworks.com/ (The Math Works, Inc., 2020).

#### **Declarations**

**Competing interests** The authors declare that they have no competing financial interests or personal relationships that could influence the work reported in this paper.

### References

- Akyurek Z, Kuter S, Karaman ÇH, Akpınar B (2023) Understanding the snow cover climatology over Turkey from ERA5-Land reanalysis data and MODIS snow cover frequency product. Geosciences 13(10):311. https://doi.org/10.3390/geosciences13100311
- Beck HE, Pan M, Miralles DG, Reichle RH, Dorigo WA, Hahn S, Sheffield J et al (2021) Evaluation of 18 satellite- and modelbased soil moisture products using in situ measurements from 826 sensors. Hydrol Earth Syst Sci 25:17–40. https://doi.org/10. 5194/hess-25-17-2021
- Cao J, Lu RY, Hu JM, Wang H (2013) Spring Indian Ocean-western Pacific SST contrast and the East Asian summer rainfall

- anomaly. Adv Atmos Sci 30:1560–1568. https://doi.org/10.1007/s00376-013-2298-6
- Cao F, Gao T, Dan L, Ma Z, Yang X, Yang F (2018) Contribution of large-scale circulation anomalies to variability of summer precipitation extremes in northeast China. Atmos Sci Lett 19:e867. https://doi.org/10.1002/asl.867
- Chen Z, Zhang J (2020) The characteristics of late summer extreme precipitation in northern China and associated large-scale circulations. Int J Climatol 40:5170–5187. https://doi.org/10.1002/joc.6512
- Cheng F, Li Q, Wang J et al (2022) Interdecadal Variability of Spring Eurasian Snowmelt and Its Impact on Eastern China Summer Precipitation. J Frontiers in Earth Science 10:927876. https:// doi.org/10.3389/feart.2022.927876
- Choi YW, Ahn JB (2019) Possible mechanisms for the coupling between late spring sea surface temperature anomalies over tropical Atlantic and East Asian summer monsoon. Clim Dyn 53:6995–7009. https://doi.org/10.1007/s00382-019-04970-3
- Choi KS, Wu CC, Cha EJ (2010) Change of tropical cyclone activity by Pacific-Japan teleconnection pattern in the western North Pacific. Journal of Geophysical Research: Atmospheres 115:D19114. https://doi.org/10.1029/2010JD013866
- Cohen J, Rind D (1991) The Effect of Snow Cover on the Climate.

  J Clim 4:689–706. https://doi.org/10.1175/1520-0442(1991)
  004%3c0689:TEOSCO%3e2.0.CO;2
- Dang H, Jian Z, Wang Y, Mohtadi M et al (2020) Pacific warm pool subsurface heat sequestration modulated Walker circulation and ENSO activity during the Holocene. Sci Adv 6(42):eabc0402. https://doi.org/10.1126/sciadv.abc0402
- Ding YH, Wang ZY, Sun Y (2008) Inter-decadal variation of the summer precipitation in East China and its association with decreasing Asian summer monsoon. Part I: observed evidences. Int J Climatol 28:1139–1161. https://doi.org/10.1002/Joc.1615
- Dirmeyer PA, Halder S (2017) Relation of Eurasian Snow Cover and Indian Summer Monsoon Rainfall: Importance of the Delayed Hydrological Effect. J Clim 30:1273–1289. https://doi.org/10.1175/JCLI-D-16-0033.1
- Du MX, Lin ZD, Lu RY (2016) Inter-decadal Change in the Summertime Northeast Asia Low-Pressure System in the Early 1990s.
  J Chin J Atmos Sci (in Chinese) 40:805–816. https://doi.org/ 10.3878/j.issn.1006-9895.1511.15178
- Du Y, Zhang J, Zhao S et al (2022a) A mechanism of spring Barents Sea ice effect on the extreme summer droughts in northeastern China. Clim Dyn 58:1033–1048. https://doi.org/10.1007/ s00382-021-05949-9
- Du Y, Xie Z, Wang N, Miao Q, Zhang L (2022b) Influence of Zonal Variation of the Subtropical Westerly Jet on Rainfall Patterns and Frequency of Heavy Precipitation Events over East Asia. J Climate 35:6611–6626. https://doi.org/10.1175/ JCLI-D-21-0872.1
- Fang Y et al (2018) The remote responses of early summer cold vortex precipitation in northeastern China compared with the previous sea surface temperatures. Atmos Res 214:399–409. https://doi.org/10.1016/j.atmosres.2018.08.007
- Feng J, Li J (2011) Influence of El Niño Modoki on spring rainfall over south China. J Geophys Res 116:D13102. https://doi.org/10.1029/2010JD015160
- Feng J, Chen W, Li YJ (2017) Asymmetry of the winter extra-tropical teleconnections in the Northern Hemisphere associated with two types of ENSO. J Climate Dyn 48:2135–2151. https://doi.org/10.1007/s00382-016-3196-2
- Gao J, Gao H (2018) Influence of the Northeast Cold Vortex on Flooding in Northeast China in Summer 2013. Journal of Meteorological Research 32(2):172–180. https://doi.org/10.1007/ s13351-018-7056-3
- Gong H, Wang L, Chen W, Wu R, Huang G, Nath D (2018) Diversity of the Pacific-Japan Pattern among CMIP5 Models: Role of SST



- Anomalies and Atmospheric Mean Flow. J Climate 31:6857–6877. https://doi.org/10.1175/JCLI-D-17-0541.1
- Guo D, Gao Y, Bethke I et al (2014) Mechanism on how the spring Arctic sea ice impacts the East Asian summer monsoon. Theoret Appl Climatol 115:107–119. https://doi.org/10.1007/s00704-013-0872-6
- Han TT, Chen H, Wang H (2015) Recent changes in summer precipitation in Northeast China and the background circulation. J Int J Climatol 35(14):4210–4219. https://doi.org/10.1002/joc.4280
- Han TT, Wang H, Sun J (2017) Strengthened relationship between eastern ENSO and summer precipitation over Northeast China. J Climate 30:4497–4512. https://doi.org/10.1175/JCLI-D-16-0551.1
- Han T, He S, Wang H et al (2019) Variation in Principal Modes of Midsummer Precipitation over Northeast China and Its Associated Atmospheric Circulation. Adv Atmos Sci 36:55–64. https:// doi.org/10.1007/s00376-018-8072-z
- Han TT, Zhang M, Zhu J et al (2021) Impact of early spring sea ice in Barents Sea on midsummer rainfall distribution at Northeast China. J Clim Dyn 57:1023–1037. https://doi.org/10.1007/ s00382-021-05754-4
- He J, Wu Z, Jiang Z et al (2007) "Climate effect" of the northeast cold vortex and its influences on Meiyu. Chin Sci Bull 52:671–679. https://doi.org/10.1007/s11434-007-0053-z
- Hersbach H, Bell B, Berrisford P, Hirahara S, Horányi A, Muñoz-Sabater J et al (2020) The ERA5 global reanalysis. Q J R Meteorol Soc 146(730):1999–2049. https://doi.org/10.1002/qj.3803
- Honda M, Inoue J, Yamane S (2009) Influence of low Arctic sea-ice minima on anomalously cold Eurasian winters. Geophys Res Lett 36:L08707, https://doi.org/10.1029/2008GL037079
- Hu KX, Lu RY, Wang DH (2011) Cold Vortex over Northeast China and Its Climate Effect[J]. Chin J Atmos Sci 35(1):179–191. https://doi.org/10.3878/j.issn.1006-9895.2011.01.15
- Hu KM, Huang G, Wu RG et al (2018) Structure and dynamics of a wave train along the wintertime Asian jet and its impact on East Asian climate. J Climate Dyn 51(11):4123–4137. https://doi.org/ 10.1007/s00382-017-3674-1
- Hu P, Feng G, Dogar MM et al (2020) Joint Effect of East Asia-Pacific and Eurasian Teleconnections on the Summer Precipitation in North Asia. J Meteorol Res 34:559–574. https://doi.org/10.1007/ s13351-020-9112-z
- Huang G (2004) An index measuring the interannual variation of the East Asian summer monsoon—The EAP index. Adv Atmos Sci 21:41–52. https://doi.org/10.1007/BF02915679
- Huang RH, Li WJ (1988) Influence of heat source anomaly over the western tropical Pacific on the subtropical high over East Asia and its physical mechanism. Chin J Atmos Sci 12:107–116. https://doi.org/10.3878/j.issn.1006-9895.1988.t1.08
- Jia X, Cao DR, Ge JW, Wang M (2018) Interdecadal change of the impact of Eurasian snow on spring precipitation over southern China. J Geophys Res: Atmos 123(18):10–092. https://doi.org/ 10.1029/2018JD028612
- Li YF, Leung LR (2013) Potential impacts of the arctic on interannual and interdecadal summer precipitation over China. J Clim 26(3):899–917. https://doi.org/10.1175/JCLI-D-12-00075.1
- Li F, Wang H (2013) Relationship between Bering Sea ice cover and East Asian winter monsoon year-to-year variations. Adv Atmos Sci 30:48–56. https://doi.org/10.1007/s00376-012-2071-2
- Li H, Chen H, Wang H, Sun J, Ma J (2018) Can Barents Sea Ice Decline in Spring Enhance Summer Hot Drought Events over Northeastern China? J Climate 31:4705–4725. https://doi.org/ 10.1175/JCLI-D-17-0429.1
- Li H, He S, Gao Y, Chen H, Wang H (2020a) North Atlantic Modulation of Interdecadal Variations in Hot Drought Events over Northeastern China. J Climate 33:4315–4332. https://doi.org/10.1175/JCLI-D-19-0440.1

- Li M, Wu P, Ma Z (2020b) A comprehensive evaluation of soil moisture and soil temperature from third-generation atmospheric and land reanalysis data sets. Int J Climatol 40:5744–5766. https://doi.org/10.1002/joc.6549
- Li H, Sun B, Wang H, Zhou B, Duan M (2022) Mechanisms and physical-empirical prediction model of concurrent heatwaves and droughts in July–August over northeastern China. J Hydrol 614:128535. https://doi.org/10.1016/j.jhydrol.2022.128535
- Liang L, Li L, Liu Q (2011) Precipitation variability in Northeast China from 1961 to 2008. J Hydrol 404(1–2):67–76. https://doi.org/10.1016/j.jhydrol.2011.04.020
- Liu X, Michio Y (2002) Influence of Eurasian spring snow cover on Asian summer rainfall. Int J Climatol 22(9):1075–1089. https://doi.org/10.1002/joc.784
- Liu X, Yanai M (2002) Influence of Eurasian spring snow cover on Asian summer rainfall. Int J Climatol: J R Meteorol Soc 22(9):1075–1089. https://doi.org/10.1002/joc.784
- Liu ZX, Lian Y, Gao ZT, Sun L, Shen BZ (2002) Analyses of the Northern Hemisphere Circulation Characters during Northeast Cold Vortex Persistence. Chin J Atmos Sci 26(3):361–372. https://doi.org/10.3878/j.issn.1006-9895.2002.03.07
- Liu HB, Wen M, He JH, Zhang RH (2012) Characteristics of the Northeast Cold Vortexat Intraseasonal Time Scale and Its Impact. Chin J Atmos Sci 36(5):959–973. https://doi.org/10.3878/j.issn.1006-9895.2012.11167
- Liu Y, Zhang M, Wu R (2016) Soil moisture-precipitation feedback in the western United States. Journal of Geophys Res: Atmos 121(22):13086–13102. https://doi.org/10.1002/2016JD025265
- Liu L, Zhang RH, Zuo ZY (2017) Effect of spring precipitation on summer precipitation in eastern China: Role of soil moisture. J Clim 30(22):9183–9194. https://doi.org/10.1175/JCLI-D-17-0028.1
- Liu Y, Sun X, Yang XQ (2023) Stage-dependent influence of PDO on interdecadal summer precipitation anomalies in eastern China. Clim Dyn 61:2071–2084. https://doi.org/10.1007/ s00382-023-06667-0
- Lu JM et al (2006) Differences of Influences of Tropical Western Pacific SST Anomaly and Rossby Wave Propagation on East Asian Monsoon in the Summers of 1993 and 1994. Chin J Atmos Sci 30(5):977–987. https://doi.org/10.3878/j.issn.1006-9895. 2006.05.25
- Lu J, Vecchi GA, Reichler T (2007) Expansion of the Hadley cell under global warming. Geophys Res Lett 34:L06805. https://doi.org/ 10.1029/2006GL028443
- Lu MM, Wu RG, Yang S, Wang ZB (2020) Relationship between Eurasian cold-season snows and Asian summer monsoons: regional characteristics and seasonality. Trans Atmos Sci 43(1):93–103. https://doi.org/10.13878/j.cnki.dqkxxb.20191025001
- McPhaden MJ, Zebiak SE, Glantz MH (2006) ENSO as an integrating concept in earth science. Science 314(5806):1740–1745. https://doi.org/10.1126/science.1132588
- Mortimer C, Mudryk L, Derksen C, Luojus K, Brown R, Kelly R, Tedesco M (2020) Evaluation of long-term Northern Hemisphere snow water equivalent products. Cryosphere 14(5):1579–1594. https://doi.org/10.5194/tc-14-1579-2020
- Muñoz-Sabater J, Dutra E, Agustí-Panareda A, Albergel C et al (2021) ERA5-Land: A state-of-the-art global reanalysis dataset for land applications. Earth System Science Data 13(9):4349–4383. https://doi.org/10.5194/essd-13-4349-2021
- Nitta T (1987) Convective activities in the tropical western Pacific and their impact on the Northern Hemisphere summer circulation. J Meteorol Soc Japan Ser II 65(3):373–390. https://doi.org/10. 2151/jmsj1965.65.3\_373
- Nitta T, Hu ZZ (1996) Summer climate variability in China and its association with 500 hPa height and tropical convection. J Meteorol Soc Japan Ser II 74:425–445. https://doi.org/10.2151/jmsj1965.74.4\_425



- Petoukhov V, Semenov V (2010) A link between reduced Barents-Kara sea-ice and cold winter extremes over northern continents. J Geophys Res 115:D21111. https://doi.org/10.1029/2009JD013568
- Pierrehumbert RT (2000) Climate change and the tropical Pacific: The sleeping dragon wakes. Proc Natl Acad Sci 97(4):1355–1358. https://doi.org/10.1073/pnas.97.4.135
- Shen Y, Xiong A, Wang Y, Xie P (2010) Performance of high-resolution satellite precipitation products over China. J Geophys Res 115:D02114. https://doi.org/10.1029/2009JD012097
- Si D, Jiang D, Hu A, Lang X (2021) Variations in northeast Asian summer precipitation driven by the Atlantic multidecadal oscillation. Int J Climatol 41:1682–1695. https://doi.org/10.1002/joc.6912
- Sun L, An G (2001) A diagnostic study of Northeast cold vortex heavy rain over the Songhuajiang-Nenjiang River basin in the summer of 1998. Chin J Atmos Sci (in Chinese) 25(3):342–354. https:// doi.org/10.3878/j.issn.1006-9895.2001.03.05
- Sun J, Wang H (2006) Regional difference of summer air temperature in Northeast China and its relationship to atmospheric general circulation and sea surface temperature (in Chinese). Chin J Geophys 49(3):662–671. https://doi.org/10.1002/cjg2.872
- Sun C, Li J, Zhao S (2015) Remote influence of Atlantic multidecadal variability on Siberian warm season precipitation. Sci Rep 5(1):16853. https://doi.org/10.1038/srep16853
- Sun L, Shen BZ, Sui B, Huang BH (2017) The influences of East Asian summer monsoon on summer precipitation in Northeast China. Clim Dyn 48:1657–1659. https://doi.org/10.1007/ s00382-016-3165-9
- Sun B, Wang H, Zhou B (2019) Interdecadal Variation of the Relationship between East Asian Water Vapor Transport and Tropical Pacific Sea Surface Temperatures during January and Associated Mechanisms. J Climate 32:7575–7594. https://doi.org/10.1175/ JCLI-D-19-0290.1
- Sun Y, Chen H, Zhu S, Zhang J, Wei J (2021a) Influence of the Eurasian Spring Snowmelt on Summer Land Surface Warming over Northeast Asia and its Associated Mechanism. J Clim 34(12):1–65. https://doi.org/10.1175/JCLI-D-20-0756.1
- Sun L, Yang X, Tao L, Fang J, Sun X (2021b) Changing Impact of ENSO Events on the Following Summer Rainfall in Eastern China since the 1950s. J Climate 34:8105–8123. https://doi.org/ 10.1175/JCLI-D-21-0018.1
- Tabari H (2020) Climate change impact on flood and extreme precipitation increases with water availability. Sci Rep 10:13768. https://doi.org/10.1038/s41598-020-70816-2
- Takaya K, Nakamura H (2001) A Formulation of a Phase-Independent Wave-Activity Flux for Stationary and Migratory Quasigeostrophic Eddies on a Zonally Varying Basic Flow. J Atmos Sci 58:608–627. https://doi.org/10.1175/1520-0469(2001)058% 3c0608:AFOAPI%3e2.0.CO;2
- Thackeray CW, Derksen C, Fletcher CG et al (2019) Snow and Climate: Feedbacks, Drivers, and Indices of Change. Current Climate Change Reports 5:322–333. https://doi.org/10.1007/s40641-019-00143-w
- Torti J (2012) Floods in Southeast Asia: A health priority. J Glob Health 2(2):020304. https://doi.org/10.7189/jogh.02.020304
- Varga ÁJ, Breuer H (2023) Evaluation of snow depth from multiple observation-based, reanalysis, and regional climate model datasets over a low-altitude Central European region. Theor Appl Climatol 153:1393–1409. https://doi.org/10.1007/s00704-023-04539-5
- Wakabayashi S, Kawamura R (2004) Extraction of major teleconnection patterns possibly associated with the anomalous summer climate in Japan. J Meteorol Soc Japan Ser II 82(6):1577–1588. https://doi.org/10.2151/jmsj.82.1577
- Wallace JM, Gutzler DS (1981) Teleconnections in the Geopotential Height Field during the Northern Hemisphere Winter. Mon

- Weather Rev 109(4):784–812. https://doi.org/10.1175/1520-0493(1981)109%3c0784:TITGHF%3e2.0.CO;2
- Wang B, Wu R, Fu X (2000) Pacific-East Asian Teleconnection: How Does ENSO Affect East Asian Climate? J Climate 13:1517– 1536. https://doi.org/10.1175/1520-0442(2000)013%3c1517: PEATHD%3e2.0.CO;2
- Wang DH, Zhong SX, Liu Y et al (2007) Advances in the study of rainstorm in Northeast China. Adv Earth Sci (in Chinese) 22(6):549– 560. https://doi.org/10.1002/jrs.1570
- Wang XF, He JH, Lian Y (2013) Effect of the previous anomalous heat content in the western Pacific warm pool on the summer rainfall over Northeast China. Acta Meteorol Sin 71(2):305–317. https:// doi.org/10.11676/qxxb2013.024
- Wang JK, Yu JY, Johnson KR (2020) Pacific and Atlantic controls of the relationship between Mainland Southeast Asia and East China interannual precipitation variability. Clim Dyn 54:4279–4292. https://doi.org/10.1007/s00382-020-05227-0
- Wang H, Wang S, Shu X, He Y, Huang J (2024) Increasing occurrence of sudden turns from drought to flood over China. J Geophys Res: Atmos 129(3):e2023JD039974. https://doi.org/10.1029/2023JD039974
- Wang X, Hu ZZ, Hu P, Ye J, Feng G (2023) The weakening relationship between ENSO and the following summer Pacific Japan teleconnection since the late 1990s. Clim Dyn 61:4033–4046. https://doi.org/10.1007/s00382-023-06783-x
- Wu R, Kirtman BP (2007) Observed relationship of spring and summer East Asian rainfall with winter and spring Eurasian snow. J Clim 20:1285–1304. https://doi.org/10.1175/JCLI4068.1
- Wu RG, Wang B (2002) A contrast of the East Asian summer monsoon–ENSO relationship between 1962–77 and 1978–93. J Clim 15:3266–3279. https://doi.org/10.1175/15200442(2002)015% 3c3266:ACOTEA%3e2.0.CO;2
- Wu B, Yang K, Zhang R (2009a) Eurasian snow cover variability and its association with summer rainfall in China. Adv Atmos Sci 26:31–44. https://doi.org/10.1007/s00376-009-0031-2
- Wu B, Zhang R, Wang B, D'Arrigo R (2009b) On the association between spring Arctic sea ice concentration and Chinese summer rainfall. Geophys Res Lett 36:L09501. https://doi.org/10. 1029/2009GL037299
- Wu B, Yang K, Zhang R (2011) Interannual variability of the east asian summer monsoon and its association with the anomalous atmospheric circulation over the mid-high latitudes and external forcing. Acta Meteorol Sin 69(2):219–233. https://doi.org/10.11676/qxxb2011.019
- Wu RG, Zhao P, Liu G (2014) Change in the contribution of spring snow cover and remote oceans to summer air temperature anomaly over Northeast China around 1990. J Geophys Res: Atmos 119:663–676. https://doi.org/10.1002/2013JD020900
- Wu B, Zhou T, Li T (2017) Atmospheric Dynamic and Thermodynamic Processes Driving the Western North Pacific Anomalous Anticyclone during El Niño. Part I: Maintenance Mechanisms. J Clim 30:9621–9635. https://doi.org/10.1175/JCLI-D-16-0489.1
- Wu J, Liu Y, Li YS et al (2022) The extreme Northeast China Cold Vortex activities in the late spring of 2021 and possible causes involved. Adv Clim Chang Res 13(6):787–796. https://doi.org/ 10.1016/j.accre.2022.09.002
- Xie Q, Huang SS (1990) A study of the effects of anomalies of the central-eastern equatorial Pacific sea surface temperature and the Arctic sea ice cover on the atmospheric general circulation during the northern winter (in Chinese). Sci Meteorol Sin 10:325–338
- Xie F, Ma X, Li J, Tian W, Ruan C, Sun C (2020) Using Observed Signals from the Arctic Stratosphere and Indian Ocean to Predict April–May Precipitation in Central China. J Climate 33:131–143. https://doi.org/10.1175/JCLI-D-18-0512.1
- Xu L, Dirmeyer P (2011) Snow–atmosphere coupling strength in a global atmospheric model. Geophys Res Lett 38:L13401. https:// doi.org/10.1029/2011GL048049



- Xu B, Chen H, Gao C, Zeng G, Huang Q (2021) Abnormal change in spring snowmelt over Eurasia and its linkage to East Asian summer monsoon: The hydrological effect of snow cover. Front Earth Sci 8:594546. https://doi.org/10.3389/FEART.2020.594656
- Yang K, Wang C, Bao H (2016) Contribution of soil moisture variability to summer precipitation in the northern hemisphere. J Geophys Res-Atmos 121(20):12108–12124. https://doi.org/10. 1002/2016JD025644
- Zhang L, Zhou T (2015) Drought over East Asia: a review. J Clim 28(8):3375–3399, https://doi.org/10.1175/JCLI-D-14-00259.1
- Zhang RH, Zhang RN, Zuo ZY (2016) An Overview of Wintertime Snow Cover Characteristics over China and the Impact of Eurasian Snow Cover on Chinese Climate. J Appl Meteorol Sci 27(5):513–526. https://doi.org/10.11898/1001-7313.20160501
- Zhang RN, Zhang RH, Zuo ZY (2017) Impact of Eurasian spring snow decrement on East Asian summer precipitation. J Clim 30(9):3421–3437. https://doi.org/10.1175/JCLI-D-16-0214.1
- Zhang R, Sun C, Zhang R, Li W, Zuo J (2019) Role of Eurasian snow cover in linking winter-spring Eurasian coldness to the autumn Arctic sea ice retreat. J Geophys Res: Atmos 124:9205–9221. https://doi.org/10.1029/2019JD030339
- Zhang T, Wang T, Feng Y, Li X, Krinner G (2021a) An emerging impact of Eurasian spring snow cover on summer rainfall in Eastern China. Environ Res Lett 16(5):054012. https://doi.org/10.1088/1748-9326/abf688
- Zhang T, Wang T, Zhao Y, Xu C, Feng Y, Liu D (2021b) Drivers of Eurasian Spring Snow-Cover Variability. J Climate 34:2037–2052. https://doi.org/10.1175/JCLI-D-20-0413.1
- Zhang S, Zeng G, Yang X et al (2022a) Connection between interannual variation of spring precipitation in Northeast China and preceding winter sea ice over the Barents Sea. Int J Climatol 42(3):1922–1936. https://doi.org/10.1002/joc.7343
- Zhang M, Sun J, Gao Y (2022b) Impacts of North Atlantic sea surface temperature on the predominant modes of spring precipitation monthly evolution over Northeast China. Clim Dyn 58(5–6):1383–1401. https://doi.org/10.1007/s00382-021-05966-8
- Zhang J, Wang S, Huang J, He Y, Ren Y (2023) The precipitation-recycling process enhanced extreme precipitation in Xinjiang, China. Geophys Res Lett 50:e2023GL104324. https://doi.org/ 10.1029/2023GL104324
- Zhao P, Zhang X, Zhou X, Ikeda M, Yin Y (2004) The Sea Ice Extent Anomaly in the North Pacific and Its Impact on the East Asian

- Summer Monsoon Rainfall. J Clim 17:3434–3447. https://doi.org/10.1175/1520-0442(2004)017%3c3434:TSIEAI%3e2.0.CO;2
- Zhao J, Zhou J, Yang L, Hou W, Feng G (2018) Inter-annual and interdecadal variability of early- and late-summer precipitation over northeast China and their background circulation. Int J Climatol 38:2880–2888. https://doi.org/10.1002/joc.5470
- Zhao J, Zhou J, Xiong K et al (2019) Relationship between Tropical Indian Ocean SSTA in Spring and Precipitation of Northeast China in Late Summer. J Meteorol Res 33:1060–1074. https://doi.org/10.1007/s13351-019-9026-9
- Zhao YX, Li J, Zhang L et al (2023) Diurnal cycles of cloud cover and its vertical distribution over the Tibetan Plateau revealed by satellite observations, reanalysis datasets, and CMIP6 outputs. Atmos Chem Phys 23(1):743–769
- Zhao Y, Li J, Wang Y, Zhang W, Wen D (2024) Warming climateinduced changes in cloud vertical distribution possibly exacerbate intra-atmospheric heating over the Tibetan Plateau. Geophys Res Lett 51(3):e2023GL107713
- Zong H, Zhang Q, Chen L (2008) A study of the process of East Asia-Pacific teleconnection pattern formation and the relationship to ENSO (in Chinese). Chin J Atmos Sci 32:220–230. https://doi.org/10.3878/j.issn.1006-9895.2008.02.03
- Zuo Z, Zhang R (2007) The spring soil moisture and the summer rainfall in eastern China. Chin Sci Bull 52:3310–3312. https://doi.org/10.1007/s11434-007-0442-3
- Zuo Z, Zhang R (2016) Influence of soil moisture in eastern China on the East Asian summer monsoon. Adv Atmos Sci 33:151–163. https://doi.org/10.1007/s00376-015-5024-8
- Zuo Z, Zhang R, Wu B, Rong X (2012) Decadal variability in springtime snow over Eurasia: Relation with circulation and possible influence on springtime rainfall over China. Int J Climate 32:1336–1345. https://doi.org/10.1002/joc.2355

**Publisher's Note** Springer Nature remains neutral with regard to jurisdictional claims in published maps and institutional affiliations.

Springer Nature or its licensor (e.g. a society or other partner) holds exclusive rights to this article under a publishing agreement with the author(s) or other rightsholder(s); author self-archiving of the accepted manuscript version of this article is solely governed by the terms of such publishing agreement and applicable law.

